Inorganic Chemistry

Article

pubs.acs.org/IC

A Neutral Cluster Cage with a Tetrahedral $[Pd^{II}_{12}L_6]$ Framework: Crystal Structures and Host–Guest Studies

Arvind K. Gupta, Ashok Yadav, Anant Kumar Srivastava, Kormathmadam Raghupathy Ramya, Harshad Paithankar, Shyamapada Nandi, Jeetender Chugh,* and Ramamoorthy Boomishankar*

Department of Chemistry, Indian Institute of Science Education and Research (IISER), Pune, Dr. Homi Bhabha Road, Pune 411008, India

Supporting Information

ABSTRACT: A charge-neutral tetrahedral $[(Pd_3X)_4L_6]$ cage assembly built from a trinuclear polyhedral building unit (PBU), $[Pd_3X]^{3+}$, cis-blocked with an imido P(V) ligand, $[(N^iPr)_3PO]^{3-}$ (X^{3-}), and oxalate dianions (L^{2-}) is reported. Use of benzoate or ferrocene dicarboxylate anions, which do not offer wide-angle chelation as that of oxalate dianions, leads to smaller prismatic clusters instead of polyhedral cage assemblies. The porosity of the tetrahedral cage assembly was determined by gas adsorption studies, which show a higher uptake capacity for CO_2 over N_2 and H_2. The tetrahedral cage was shown to encapsulate a wide range of neutral guest solvents from polar to nonpolar such as dimethyl sulfoxide, benzene, dichloromethane, chloroform, carbon tetrachloride, and cyclopentane as observed by mass spectral and single-crystal X-ray diffraction studies. The ^1H two-dimensional diffusion ordered spectroscopy NMR analysis shows that the host and guest molecules exhibit similar diffusion coefficients in all the studied host–guest systems. Further, the tetrahedral cage shows selective binding of benzene, CCl_4, and cyclopentane among other solvents from their categories as evidenced from mass spectral analysis. A preliminary density functional theory analysis gave a highest binding energy for benzene among the other solvents that were structurally shown to be encapsulated at the intrinsic cavity of the tetrahedral cage.

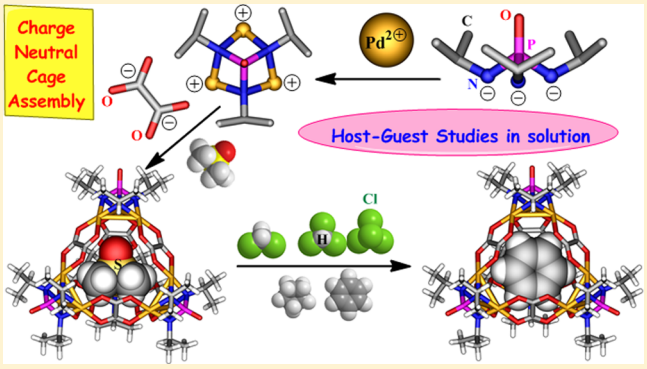

INTRODUCTION

Over the years, self-assembled molecular architectures derived from abiological systems have evolved into an intense field of research in supramolecular chemistry.[1] Synthetic approaches to artificial assemblies involve the use of small and simple molecular building blocks, which react in a cooperative manner to yield highly organized structures.[2] Besides their structural novelty, these assemblies reveal promising applications in host–guest chemistry, namely, guest recognition, storage, chemical sensing, protection and entrapment of reactive molecules, and catalysis in their confined space.[3] Polyhedral cages derived from metal–ligand coordination bonds belong to one such notable class of self-assembled systems among several known supramolecular entities.[4] Most often these were obtained as cationic or anionic assemblies by choosing geometrically tailored metal ions as nodes and organic ligands as directional bridging motifs.[5,6] Conversely, in recent years tremendous attention has been accorded to the use of multimetallic scaffolds or clusters as vertices for obtaining charge-neutral nanocages that are termed as metal–organic polyhedra (MOPs).[7] However, rational routes to access these kinds of MOPs have been restricted to a small number of systems, namely, the dimetallic "paddle-wheel" motifs of formula $[M_2(COO)_4]$,[7a−d] the M_4-thiacalix-[4]arane "shuttle cock"-shaped subunits,[7e−g] and certain polyoxometallates.[7h] This could be attributed to (a) the lack of precise control over the reactivity of such cluster motifs favoring the formation of extended two- or three-dimensional structures[8] and (b) the limited availability of suitable auxiliary groups[9] that can specifically protect some of the metal-coordination sites in these clusters for the exclusive formation of MOPs. Recently, we developed a synthetic approach for accessing tris(amido)phosphate trianions of the type $[PO(NR)_3]^{3-}$ in polar protic medium as hexanuclear Pd(II) complexes of composition $\{Pd_3[(NR)_3PO](OAc)_3\}_2$ or $\{Pd_3[(NR)_3PO](OAc)_2(OR')\}_2$ in which the acetate groups act as bridging ligands between two trinuclear $\{Pd_3[(NR)_3PO]\}^{3+}$ motifs.[10] Spurred by the unique cis coordination of the $[(NR)_3PO]^{3-}$ ligand to the trinuclear Pd(II) centers, we envisioned that polyhedral cages based on these Pd_3 motifs could be built by replacement of the acetate bridges in these clusters with suitably chosen carboxylate linkers. Herein, by employing oxalate linkers, we show the formation of an interesting charge-neutral tetrahedral cage assembly in which the $[Pd_3(N^iPr)_3PO]^{3+}$ moiety, denoted as $[Pd_3X]^{3+}$ (X^{3-} = $[(N^iPr)_3PO]^{3-}$), acts as a polyhedral building

Received: November 21, 2014
Published: March 17, 2015

DOI: 10.1021/ic502798r
Inorg. Chem. 2015, 54, 3196−3202

unit (PBU). However, the prismatic cluster assembly of the precursor was retained when benzoate or 1,1′-ferrocene dicarboxylate (FDC) moieties were employed in these ligand-substitution reactions, exemplifying the need of large-angle chelating linkers for obtaining polyhedral cages based on these PBUs (Scheme 1).

Scheme 1. Formation of the Cage Assembly of 2 and Prismatic Clusters 3 and 4[a]

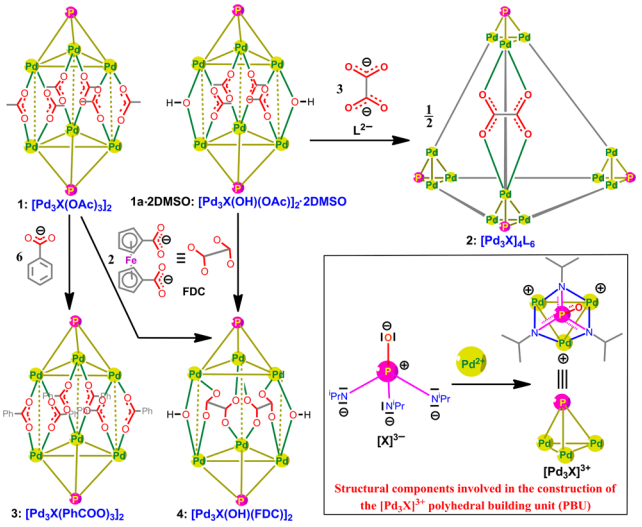

[a]Only one of the six oxalate linkers is shown for **2**.

EXPERIMENTAL SECTION

General Remarks. All manipulations involving phosphorus halides were performed under dry nitrogen atmosphere in standard Schlenk glassware. Solvents were dried over potassium (tetrahydrofuran, hexane) and sodium (toluene). The primary amines, oxalic acid, and ferric oxalate hexahydrate were purchased from Aldrich and used as received. $POCl_3$ was purchased locally and was distilled prior to use. NMR spectra were recorded on a Jeol 400 MHz spectrometer (^{1}H NMR: 400.13 MHz, ^{13}C{^{1}H}NMR: 100.62 MHz, ^{31}P{^{1}H} NMR: 161.97 MHz) or on a Bruker 500 MHz (^{1}H NMR: 500.00 MHz, ^{13}C{^{1}H}NMR: 125.725 MHz, ^{31}P{^{1}H} NMR: 202.404 MHz) spectrometer at room temperature using $SiMe_4$ (^{1}H, ^{13}C) and 85% H_3PO_4 (^{31}P). The mass spectra were obtained on an Applied Biosystem matrix-assisted laser desorption ionization time-of-flight (MALDI-TOF)/TOF spectrometer. The powder X-ray diffraction (XRD) data were obtained from a Bruker D8 Advance diffractometer. Thermal analysis data were obtained from a PerkinElmer STA-6000 thermogravimetric analyzer (TGA). Fourier transform infrared (FT-IR) spectra were taken on a PerkinElmer spectrophotometer with samples prepared as KBr pellets. Melting points were obtained using an Electrothermal melting point apparatus and were uncorrected.

Synthesis. *Preparation of Tetrahedral Cage (DMSO⊂2).* To a stirred solution of **1**·2DMSO (20 mg, 0.013 mmol, DMSO = dimethyl sulfoxide) in methanol (2 mL), oxalic acid (3 mg, 0.027 mmol) was added, and the solution was heated at 80 °C for 30 min to give an orange-colored precipitate. The resulting mixture was filtered, and the residue was washed with 10 mL portions of methanol and dried under vacuum overnight. Yield of DMSO⊂**2** (⊂ denotes encapsulation) 95% (17 mg, based on P). mp 232−234 °C. ^{1}H NMR (400 MHz, {$(CD_3)_2SO$}): δ 1.78 (br, 72H, CH_3), 2.55 (s, 6H, CH_3), 2.94 (br, 12H, CH): ^{13}C{^{1}H} (100 MHz, {$(CD_3)_2SO$}): δ 31.20, 42.20, 51.38, 174.23: ^{31}P{^{1}H} NMR (161 MHz, {$(CD_3)_2SO$}): δ 73.57 ; FT-IR data in KBr pellet (cm^{-1}): 3451, 2966, 2926, 1638, 1497, 1409, 1384, 1353,1309, 1268, 1138, 1020, 802, 722, 659. Anal. Calcd for $C_{50}H_{90}N_{12}O_{29}P_4SPd_{12}$: C, 21.79; H, 3.29; N, 6.10. Found: C, 21.98; H, 3.58; N, 6.20%. Single crystals suitable for X-ray diffraction analysis were obtained from slow evaporation of its solution in DMSO.

*Preparation of the Dimethyl Sulfoxide-Free Tetrahedral Cage (**2**$_{free}$).* To a stirred solution of [$OP(NH^iPr)_3$] (20 mg, 0.09 mmol) in methanol (5 mL), palladium acetate $Pd(OAc)_2$ (60 mg, 0.27 mmol) and oxalic acid (12 mg, 0.14 mmol) were added, and the solution was heated at 60 °C for 30 min and filtered to give an orange-colored precipitate of CH_3OH⊂**2** as evidenced by mass spectroscopy and single-crystal X-ray analysis. This was washed with three 10 mL portions of methanol and dried under vacuum overnight to yield the guest-free cage **2**$_{free}$. Yield 90% (54 mg, based on P). mp 228−230 °C, ^{1}H NMR (400 MHz, {$(CH_3)_2CO$}): δ 1.78 (d, 72H, $CH3$), 2.90 (m, 12H, CH): ^{13}C{1H} (100 MHz, {$(CH_3)_2CO$}): δ 25.78, 54.10, 174: ^{31}P{1H} NMR (161 MHz, {$(CH_3)_2CO$}): δ 72.82; FT-IR data in KBr pellet (cm^{-1}): 3457, 2962, 2933, 1618, 1507, 1429, 1394, 1363,1313, 1262, 1151, 1080, 819, 733, 657. Anal. Calcd for $C_{48}H_{84}N_{12}O_{28}P_4Pd_{12}$: C, 21.53; H, 3.16; N, 6.28. Found: C, 21.71; H, 3.19; N, 6.18%.

3. To a solution of **1** (20 mg, 0.015 mmol) in methanol, benzoic acid C_6H_5COOH (10 mg, 0.08 mmol) in methanol was added, and the solution was stirred for 1 h and kept for crystallization. Platelike orange-colored crystals were obtained after 7 d. Yield: 81% (22 mg) mp 215−217 °C. ^{1}H NMR (400 MHz, {$(CD_3)_2SO$}): δ 1.73 (d, 72H, CH_3), 2.02 (m, 12H, CH), 7.73 (dd, 2H, CH), 7.81 (dd, 3H, CH), 8.05 (dd, 3H, CH): ^{13}C{^{1}H} (100 MHz, {$(CD_3)_2SO$}): δ 25.78, 54.10, 127.32, 128.01, 136.53, 138.89: ^{31}P{^{1}H} NMR (161 MHz, {$(CD_3)_2SO$}): δ 72.82; FT-IR data in KBr pellet (cm^{-1}): 674, 694, 731, 753, 786, 864, 954, 1025, 1136, 1176, 1265, 1353, 1409, 1452, 1572, 1612, 2977, and 3423. Anal. Calcd for $C_{60}H_{72}N_6O_{14}P_2Pd_6$: C, 40.00; H, 4.03; N, 4.66. Found: C, 40.21; H, 4.13; N, 4.22%.

4. To a solution of **1**·2DMSO (20 mg, 0.013 mmol) in methanol (2 mL), 1,1-ferrocenedicarboxylic acid $Fe(C_5H_4COOH)_2$ (7.12 mg, 0.026 mmol) in methanol/DMSO (0.5 mL/0.5 mL) was added. The mixture was stirred for 1 h, filtered, and kept for crystallization. Dark orange-colored crystals were obtained in 10 d. Yield: 60% (13 mg) mp: 225−227 °C. ^{1}H NMR (400 MHz, {$(CD_3)_2SO$}): δ 1.70 (br, 72H, CH_3), 2.91(m, 12H, CH), 3.55(br, 4H, CH), 6.38(dd, 8H, CH), 6.63 (dd, 8H, CH): ^{13}C{^{1}H} (100 MHz, {$(CD_3)_2SO$}): δ 31.44, 42.20, 50.47, 130.05,132.42, 177.83: ^{31}P{^{1}H} NMR (161 MHz, {$(CD_3)_2SO$}): δ 74.99; FT-IR data in KBr pellet (cm^{-1}): 539, 669, 745, 953, 1021, 1141, 1198, 1257, 1317, 1364, 1401, 1437, 1490, 1588, 1652, and 3386. Anal. Calcd for $C_{42}H_{58}N_6O_{12}P_2Fe_2Pd_6$: C, 30.55; H, 3.54; N, 5.09. Found: C, 30.21; H, 3.73; N, 5.22%.

General procedure for preparation of Guest⊂**2** (Guests: benzene, CCl_4, $CHCl_3$, CH_2Cl_2, and C_5H_{10}) and Guest⊄**2** (toluene, chlorobenzene, fluorobenzene, and cyclohexane): DMSO⊂**2** (10 mg, 0.004 mmol) was dissolved in 2 mL of the guest solvent and stirred at a warm temperature of ∼35−40 °C until the solvents were evaporated to almost dryness. The precipitated orange-colored solid was washed with dry hexane and recovered from the reaction vessel. Single crystals of C_6H_6⊂**2**, $CHCl_3$⊂**2**, CH_2Cl_2⊂**2**, C_7H_8⊄**2**, C_6H_5Cl⊄**2**, and C_6H_5F⊄**2** suitable for XRD were obtained in a direct reaction involving **1**·2DMSO (10 mg, 0.07 mmol) and oxalic acid (1.2 mg, 0.013 mmol) in the corresponding solvents by slow evaporation. In case of CCl_4 a few drops of methanol were added for getting a homogeneous solution, and the obtained crystals of CCl_4⊂**2** were again recrystallized from CCl_4/toluene mixture for better X-ray data.

*C_6H_6⊂**2***. Yield 90% (9.1 mg, based on P). mp 224−226 °C, ^{1}H NMR (400 MHz, {$(CH_3)_2CO$}): δ 1.73 (d, 72H, CH_3), 2.90 (m, 12H, CH) 7.38 (s, 6H, CH): ^{13}C {^{1}H}} (100 MHz, {$(CH_3)_2CO$}): δ 26.90, 54.53, 133.74, 174.44: ^{31}P NMR (161 MHz, {$(CH_3)_2CO$}): δ 72.80; FT-IR data in KBr pellet (cm^{-1}): 3423, 2964, 2924, 1791, 1635, 1353, 1278, 1135, 1016, 947, 858, 804, 727, 651. Anal. Calcd for $C_{54}H_{90}N_{12}O_{28}P_4Pd_{12}$: C, 23.53; H, 3.29; N, 6.10. Found: C, 23.91; H, 3.68; N, 6.13%.

*CCl_4⊂**2***. Yield 75% (7.8 mg, based on P). mp 225−227 °C, ^{1}H NMR (400 MHz, {$(CH_3)_2CO$}): δ 1.78 (d, 72H, CH_3), 2.90 (m, 12H, CH): ^{13}C {^{1}H}} (100 MHz, {$(CH_3)_2CO$}): δ 31.21, 54.58, 99.96, 174.86: ^{31}P NMR (161 MHz, {$(CH_3)_2CO$}): δ 72.83; FT-IR data in KBr pellet (cm^{-1}): 3430, 2967, 2924, 2866, 1635,1461,1437, 1384, 1266, 1168, 1136, 1018, 951, 807, 723, 682. Anal. Calcd for

DOI: 10.1021/ic502798r
Inorg. Chem. 2015, 54, 3196−3202

$C_{49}H_{84}N_{12}O_{28}P_4Cl_4Pd_{12}$: C, 20.78; H, 2.99; N, 5.94. Found: C, 20.61; H, 2.88; N, 6.01%.

*$CHCl_3$⊂**2***. Yield 80% (8.2 mg, based on P). mp 220−222 °C, ^{1}H NMR(400 MHz, {$(CH_3)_2CO$}): δ 1.78 (d, 27H, CH_3), 2.91 (m, 9H, C*H*) 8.03 (s, 1H, C*H*): ^{13}C {^{1}H}} (100 MHz, {$(CH_3)_2CO$}): δ 27.63, 32.20, 79.67, 174.47: ^{31}P NMR (161 MHz, {$(CH_3)_2CO$}): δ 72.82; FT-IR data in KBr pellet (cm^{-1}): 3428, 2965, 1701, 1405, 1353, 1260, 1134, 1016, 946, 783, 720, 649, 570. Anal. Calcd for $C_{49}H_{85}N_{12}O_{28}P_4Cl_3Pd_{12}$: C, 21.04; H, 3.06; N, 6.01. Found: C, 21.23; H, 3.08; N, 6.13%.

*CH_2Cl_2⊂**2***. Yield 80% (8.1 mg, based on P). mp 228−230 °C, ^{1}H NMR (400 MHz, {$(CH_3)_2CO$}): δ 1.78 (d, 72H, CH_3), 2.94 (m, 12H, CH_3) 5.64 (s, 2H, CH_2): ^{13}C {^{1}H}} (100 MHz, {$(CH_3)_2CO$}): δ 31.15, 49.05, 53.34, 174.73: ^{31}P NMR (161 MHz, {$(CH_3)_2CO$}): δ 72.81; FT-IR data in KBr pellet (cm^{-1}): 3424, 2965, 1717, 1617, 1401, 1352, 1320, 1135, 1016, 948, 858, 802, 727, 650, 520. Anal. Calcd for $C_{49}H_{86}N_{12}O_{28}P_4Cl_2Pd_{12}$: C, 21.30; H, 3.14; N, 6.08. Found: C, 21.73; H, 3.48; N, 5.70%.

*C_5H_{10}⊂**2***. Yield 90% (9.1 mg, based on P). mp 203−205 °C, ^{1}H NMR (400 MHz, {$(CH_3)_2CO$}): δ 1.52 (d, 4H, CH_2), δ 1.78 (d, 72H, CH_3) 2.94 (m, 72H, CH_3), 3.80 (m, 4H, C*H*): ^{13}C {^{1}H}} (100 MHz, {$(CH_3)_2CO$}): δ 25.14, 29.68, 55.29, 174.00: ^{31}P NMR (161 MHz, {$(CH_3)_2CO$}): δ 72.80; FT-IR data in KBr pellet (cm^{-1}): 3438, 2926, 1726, 1637,1460, 1384, 1355, 1280, 1136, 1072, 996, 806, 725, 679. Anal. Calcd for $C_{53}H_{94}N_{12}O_{28}P_4Pd_{12}$: C, 23.16; H, 3.45; N, 6.12. Found: C, 23.35; H, 3.78; N, 6.23%.

Crystallography. Reflections were collected on a Bruker Smart Apex Duo diffractometer at 100 K using Mo Kα radiation (λ = 0.710 73 Å) for {DMSO⊂**2**·10DMSO·5H_2O}, C_6H_6⊂**2**, $CHCl_3$⊂**2**, CH_2Cl_2⊂**2**, C_7H_8⊄**2**, C_6H_5Cl⊄**2**, C_6H_5F⊄**2**, **3**, and **4**. For CCl_4⊂**2**, the data were collected on a Bruker D8 Venture fitted with a microfocus detector at 100 K using Cu Kα radiation (λ = 1.541 78 Å). Structures were refined by full-matrix least-squares against F^2 using all data (SHELX).[11] Crystallographic data for all these compounds are listed in Table S1 (Supporting Information). All non-hydrogen atoms were refined aniostropically if not stated otherwise. Hydrogen atoms were constrained in geometric positions to their parent atoms. Crystals of C_6H_6⊂**2**, C_7H_8⊄**2**, **3**·3H_2O, and **4**·3H_2O were weakly diffracting at higher angles, and hence a 2θ = 50° cutoff was applied. Also, the hydrogen atoms of the bridging hydroxide ions in **4**·3H_2O could not be located from the difference map. Both the encapsulated and solvated DMSO molecules in the asymmetric unit of {DMSO⊂**2**·10DMSO·5H_2O} were disordered and freely refined isotropically over two positions using similar distances and similar U-restraints. The remaining solvated atoms in it were not precisely identified and hence were refined as partially occupied water oxygen atoms. We also provided a better refined structure of this molecule (DMSO⊂**2**) with the solvated atoms in its packing cavity treated as a diffuse contribution to the overall scattering without specific atom positions by SQUEEZE/PLATON. Similarly for C_6H_6⊂**2**, CH_2Cl_2⊂**2**, $CHCl_3$⊂**2**, C_7H_8⊄**2**, C_6H_5Cl⊄**2**, and C_6H_5F⊄**2**, the encapsulated solvents were disordered and refined over two positions with SAME/SADI commands in the SHELX. The solvated atoms located at the packing cavities of C_6H_6⊂**2**, CH_2Cl_2⊂**2**, $CHCl_3$⊂**2**, CCl_4⊂**2**, C_7H_8⊄**2**, C_6H_5Cl⊄**2**, and C_6H_5F⊄**2** were treated as a diffuse contribution to the overall scattering without specific atom positions by SQUEEZE/PLATON. However, for C_7H_8⊄**2** and C_6H_5Cl⊄**2**, one molecule of each of these solvents was kept in the packing cavity. A few C, N, and O atoms in some of the structures exhibited slightly bad ellipsoids and were refined with partial isotropic parameters.

Low-Pressure Gas Sorption Studies. Low-pressure gas sorption measurements were performed using Micromeritics 3-Flex surface area and porosimetry analyzer. All the gases used were of high purity (99.9999%). To get all isotherms, ∼50 mg of the sample was activated by heating the sample at 80 °C under vacuum for 6 h and was directly loaded to the analysis port. Prior to the start of analyses, the sample was again evacuated for 2 h under turbo vacuum pump. N_2 (77 K), H_2 (77 K), and CO_2 (195, 263, 273, and 298 K) sorption isotherms were obtained for this material. Heat of adsorption for CO_2 was calculated from CO_2 adsorption isotherms (263, 273, and 298 K) using density functional theory (DFT) model; pore size distribution was calculated from 195 K CO_2 isotherm using DFT model.

NMR Spectroscopy of Guest⊂2 Systems. The NMR experiments were carried out on a Bruker NMR spectrometer operating at a ^{1}H frequency of 500 MHz and at a constant temperature of 298 K. For the measurements, 2.50 mM solution of the host cage (5 mg of $\mathbf{2}_{free}$ dissolved in 0.75 mL) in d_6-Me_2CO and 20 equiv of the respective guest solvent (∼2−4 μL) were taken and allowed to equilibrate for a period of 30 min before data acquisition. ^{1}H NMR spectra were recorded for C_6H_6, $CHCl_3$, CH_2Cl_2, DMSO, and C_5H_5 in acetone solvent in the absence and presence of **2**. Diffusion-ordered spectroscopy (DOSY) experiments were performed with a linear gradient of 24 steps between 2% and 95% of gradient strength.[12] Diffusion time (Δ) and length of the square diffusion encoding gradient pulse (δ) were optimized individually for guest and host peak in a host−guest system so that integral at 95% gradient strength drops to ∼10% of that at 2% gradient strength to obtain reliable estimates for diffusion coefficients. For benzene, this drop could not be obtained below 40% for several different values of Δ and δ. However, the value of diffusion coefficients obtained for benzene is comparable with other better optimized solvent peaks. Longitudinal relaxation time (t1) for guest and host molecules was optimized separately, and accordingly d1 (= t1 × 5) delay was used in the DOSY experiments; eight scans were recorded for each gradient step.[13] The standard Bruker protocol using Topspin 2.1 software was used for processing the DOSY data. The fitting of the diffusion dimension in the two-dimensional (2D) DOSY spectra was carried out using a two-parameter biexponential fit (eq 1) that showed better fits when compared with a two-parameter monoexponential fit.

$$I = I_{0A}\exp\left[-D_A\gamma^2 g^2\delta^2\left(\Delta - \frac{\delta}{3}\right)\right] + I_{0B}\exp\left[-D_B\gamma^2 g^2\delta^2\left(\Delta - \frac{\delta}{3}\right)\right] \quad (1)$$

In this equation, I is the observed integral, I_{0A} and I_{0B} the reference integral or unattenuated integrals, D_A and D_B the diffusion coefficients, γ the gyromagnetic ratio of the observed nucleus, g the gradient strength, δ the length of the gradient, and Δ the diffusion time.

Theoretical Calculations. DFT with dispersion-corrected B97-D[14] functional was employed for these calculations using Gaussian 09[15] software. Single-point energy calculations were performed on the crystal structures using lanl2dz basis set for palladium atom in conjunction with the cc-pVTZ basis set (for all other atoms). The binding energies for the host−guest systems as internal energies are calculated as follows

$$\text{binding energy} = E_{\text{host-guest}} - E_{\text{host}\cdots\text{guest}}$$

where $E_{\text{host-guest}}$ is the total energy of the system comprised of guest located at the center of the cage, and $E_{\text{host}\cdots\text{guest}}$ is the total energy of the system where guest is 30 Å from the center of the cage. To determine the structural changes with the encapsulation of guest in the host cage, we calculated the deformation energy,[16] and it is written as

$$\text{deformation energy} = E_{\text{host}} - E_{\text{host}}^{\text{enc}}$$

where E_{host} is the total energy of the optimized empty cage; $E_{\text{host}}^{\text{enc}}$ is obtained by removal of the guest molecule from the host cage followed by a single-point energy calculation on the corresponding structure.

RESULTS AND DISCUSSION

Syntheses. To demonstrate the general utility of ligand-substitution strategy, we chose to employ the PBU precursors[10] {$Pd_3[(N^iPr)_3PO](OAc)_3\}_2$ (**1**) or {$Pd_3[(N^iPr)_3PO]$-$(OAc)_2(OH)\}_2$·2$(CH_3)_2SO$ (**1a**·2DMSO) in reactions with various mono- and dicarboxylic acids. Thus, the reaction of oxalic acid with **1a**·2DMSO gave an interesting dodecanuclear neutral tetrahedral cage $(CH_3)_2SO$⊂{$Pd_3[(N^iPr)_3PO]_4$-$(C_2O_4)_6$}, DMSO⊂**2**. However, the reaction of benzoic acid

DOI: 10.1021/ic502798r
Inorg. Chem. 2015, 54, 3196−3202

with **1** in methanol gave the complex $\{Pd_3[(NR)_3PO]\text{-}(PhCOO)_3\}_2$ (**3**) in which the acetate groups were replaced with benzoate groups. Similar reaction of **1** or **1a**·2DMSO with 1,1′-ferrocenedicarboxylic acid (FDC-2H) in MeOH/DMSO gave the complex $\{Pd_3[(N^iPr)_3PO](FDC)(OH)\}_2$ **4**, in which four acetate bridges were replaced with two FDC bridges, and the remaining two positions were occupied by hydroxyl groups as observed for **1a**·2DMSO (Scheme 1).

The ^{31}P NMR of DMSO⊂**2** in DMSO-d_6 gave a sharp peak in the expected cluster region at δ = 73.6 ppm. The MALDI-TOF mass spectrum of DMSO⊂**2** in methanol gave two isotopic distribution of signals centered at m/z = 2717 and 2795 corresponding to $[\mathbf{2}+K]^+$ and $[DMSO⊂\mathbf{2}+K]^+$ ions, respectively. The DMSO-free cage of **2** can be obtained in a one-pot reaction involving $[(NH^iPr)_3PO]$, $Pd(OAc)_2$, and oxalic acid in methanol with the initial formation of $2CH_3OH⊂\mathbf{2}$ as evidenced by its MALDI-TOF mass spectrum. Single-crystal X-ray analysis reveals the presence of methanol (although only one disordered methanol molecule was located) inside the cavity. This was further dried in the vacuum overnight to yield the guest-free cage $\mathbf{2}_{free}$. Similarly the presence of **3** and **4** in solution was confirmed from their ^{31}P NMR and mass spectral data (Figures S1−S10, Supporting Information).

Crystal Structures. The molecular structure of DMSO⊂**2**·10DMSO·$5H_2O$ was solved from its single-crystal X-ray diffraction (SC-XRD) data in orthorhombic space group *Cmcm* (Tables S1−S3, Supporting Information). Each vertex of the cage consists of a planar cluster of three Pd(II) cations that are capped by three chelating N_{imido} sites from $[PO(N^iPr)_3]^{3-}$ (X^{3-}), trianions yielding a tetrahedral $[Pd_3X]^{3+}$ PBU. These PBUs are further connected by bridging interaction of the six oxalate (L^{2-}) ions and complete the tetrahedral cage assembly of composition $[(Pd_3X)_4L_6]$ (Figure 1a, Figure S11, Supporting Information). As described by Stang and co-workers,[17] the Pd_3 polygon acts as 60° acceptors that are linked by the 180° chelating oxalate connectors to form the tetrahedral MOP of **2**. The wide-angle chelation of the oxalate bridges are perfectly compatible with the cisoidal sites at the Pd(II) atoms to give a neatly assembled tetrahedral cage.

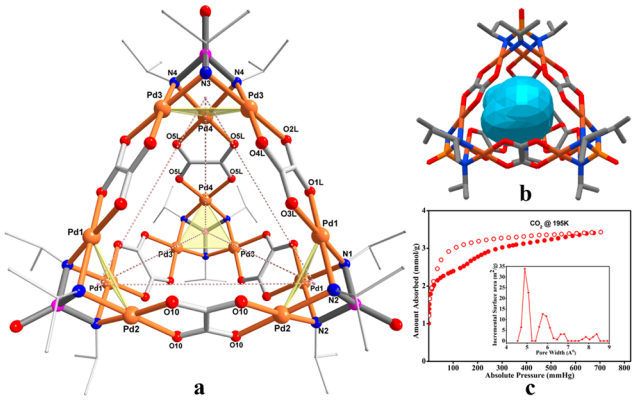

Figure 1. (a) Molecular structure of **2**. The encapsulated DMSO was omitted for clarity. (b) View of the void space inside **2** by a surface. (c) The 195 K CO_2 adsorption and desorption (open symbols) for $\mathbf{2}_{free}$. (inset) The calculated pore size distribution.

The crystal packing of DMSO⊂**2** shows two distinct types of voids: the first one is a smaller intrinsic cavity containing an encapsulated DMSO, and the second one is the larger extrinsic pore located along the *b*-axis featuring at least 10 DMSO molecules per formula unit (Figure S13, Supporting Information). The intrinsic cavity in **2** was determined by MSROLL software calculations[18a] with a fixed probe radius of 1.3 Å (Table S4, Supporting Information),[18b] which gave a cavity volume of 85.8 $Å^3$ and a cavity surface of 100.8 $Å^2$ for **2** (Figure 1b). The portals of this cage are housed along the four faces of the tetrahedron with aperture distances ranging from 3.676(1) to 8.419(1) Å (Figure S11b, Supporting Information). Considering that some nonporous tetrahedral palladium clusters are known, the host structure of **2** represents a smallest cavity cage molecule with a definite volume of 85.8 $Å^3$.[19] Although there are a few examples known for Pd(II) and Pt(II) containing neutral assemblies,[20] to the best of our knowledge, this is the first instance where multinuclear Pd(II) clusters form the vertex of a neutral polyhedron. To further establish the intrinsic porosity of **2**, gas adsorption studies for CO_2, N_2, and H_2 were undertaken for $\mathbf{2}_{free}$. (Figure 1c and Figures S14−S18, Supporting Information). The pore size distribution calculated from the 195 K CO_2 uptake profile indicates that the majority of the pores are centered around 5 Å diameters, which are closely matching with the central portal distances of **2**.

The crystal structures of **3** and **4** were solved in monoclinic space groups $P2(1)/c$ and Cc, respectively, containing the whole molecule in their asymmetric unit (Figure 2 and Figure S12, Supporting Information). The molecular core in both of them consists of a hexameric Pd_6 cluster in a prismatic geometry sandwiched between two tris(imido)phosphate ligands. In both of them, the two Pd_3 moieties of the PBUs are stacked upon each other in a closely eclipsed manner in a fashion similar to that of **1** and **1a**·2DMSO, respectively. Further, the six benzoate ligands in **3** are grouped in a set of two and connect a pair of Pd(II) atoms from the adjacent triangular units. In **4**, two of the three Pd_2 pairs possess mixed-bridged environment with one FDC moiety and one hydroxyl unit each, while the third pair contains only FDC bridges. In addition, the two ferrocenyl moieties serve as linkers (at 0° angles) to the three Pd_2 pairs and provide additional support to the prismatic structure.

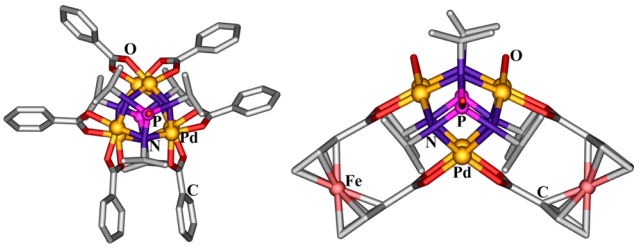

Figure 2. Molecular structures of **3** and **4**. The hydrogen atoms and the solvate molecules are omitted for clarity.

Guest-Encapsulation Studies of 2. In view of the prominent intrinsic cavity present in **2**, inclusion studies for several neutral guest solvents were performed. Thus, the encapsulated DMSO in **2** is readily exchanged with nonpolar solvents such as C_6H_6, $CHCl_3$, CH_2Cl_2, CCl_4, and C_5H_{10}, and the corresponding solvent-encapsulated cage assemblies of $C_6H_6⊂\mathbf{2}$, $CHCl_3⊂\mathbf{2}$, $CH_2Cl_2⊂\mathbf{2}$, $CCl_4⊂\mathbf{2}$, and $C_5H_{10}⊂\mathbf{2}$ were isolated as orange-colored powders (Table S5, Supporting Information). The MALDI-TOF mass spectra of all these guest included samples showing prominent isotropic distribution of

DOI: 10.1021/ic502798r
Inorg. Chem. 2015, 54, 3196−3202

peaks corresponding to $[Guest\subset\mathbf{2}+K]^+$ ions: m/z 2795 (C_6H_6), 2836 ($CHCl_3$), 2793 (CH_2Cl_2),[21] 2870 (CCl_4), and 2787 (C_5H_{10}) (Figures S19–S23, Supporting Information). The ^{1}H NMR spectra of $\mathbf{2}_{free}$ in Me_2CO-d_6 equilibrated with the respective guest solvents (20 equiv) gave only one sharp peak in the guest regions at δ = 7.38 (C_6H_6), 8.04 ($CHCl_3$), 5.64 (CH_2Cl_2), 2.55 (DMSO), and 1.52 (C_5H_{10}) ppm (Figure S24, Supporting Information). Because of the apparent overlap of the bound and free solvent signals in these ^{1}H NMR spectra, the presence of these host–guest assemblies in solution were determined by ^{1}H 2D DOSY NMR spectroscopy. For these experiments the diffusion coefficients (D) of the cage protons (^{i}Pr methyl resonance on the X^{3-} ligand) and the corresponding solvent signals were monitored (Table S6, Supporting Information). From the DOSY data analysis two diffusion coefficient values were obtained for each of the guest solvents studied: one with a faster diffusion rate attributed to the free solvent, and one with a slow diffusion rate for the bound solvent (Figure 3a,b and Figure S25, Supporting Information). Similarly, two diffusion coefficients were observed in each of these experiments for the host molecule of **2** due to free (fast-moving) and encapsulated (slow-moving) cages suggestive of a slow guest exchange in the tetrahedral assembly of **2**. The results of the DOSY experiments are summarized in Figure 3c, which clearly shows free host diffusing slower than free guest due to larger size of host. Furthermore, the bound host assembly of **2** and the corresponding solvents diffuse at almost the same rate, which confirms the encapsulation of all these five solvents inside **2**.

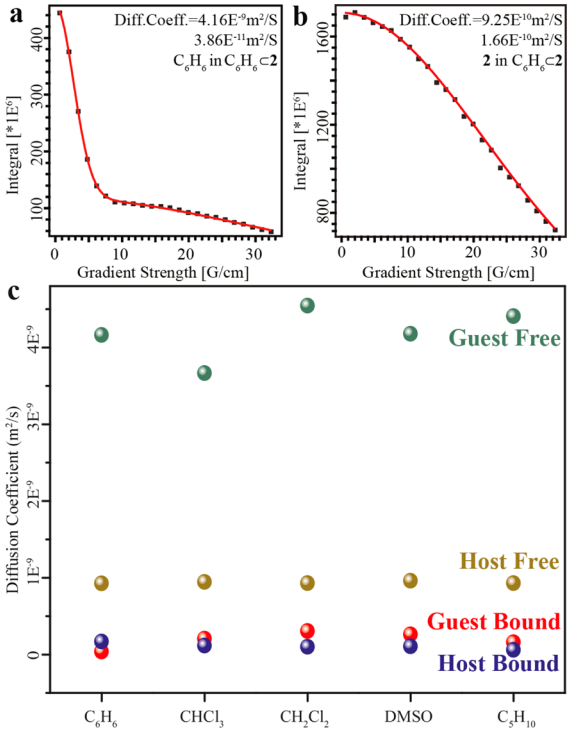

Figure 3. Integral decay profile of (a) benzene protons (δ = 7.38 ppm) and (b) ^{i}Pr methyl protons (δ = 1.78 ppm) of **2** plotted as a function of gradient strength. The dots represent experimental data, and the red line shows the best fit using eq 1. The D values obtained for free and bound host–guest systems are shown in the insets. (c) Summary of the D values for host and different guests in the studied host–guest systems.

Further, formation of $C_6H_6\subset\mathbf{2}$, $CHCl_3\subset\mathbf{2}$, $CH_2Cl_2\subset\mathbf{2}$, and $CCl_4\subset\mathbf{2}$ was confirmed from SC-XRD analyses on the crystals grown directly from the reaction mixture of **1**·2DMSO and oxalic acid in the respective solvents (Figure 4). However,

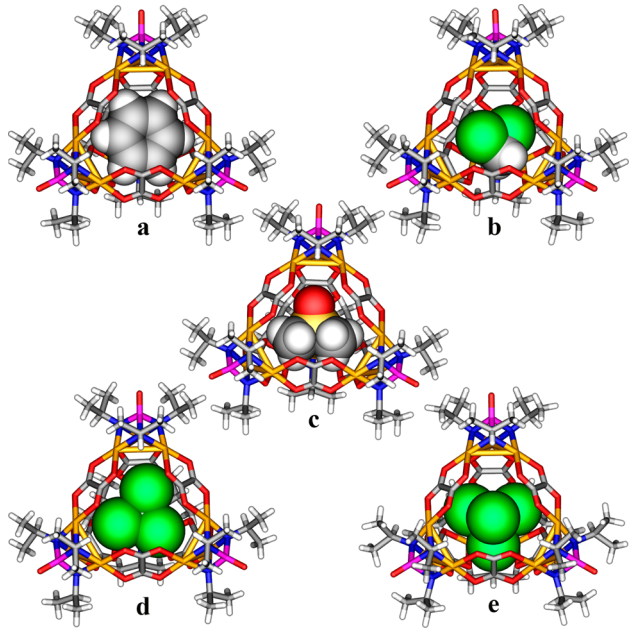

Figure 4. SC-XRD structures of (a) $C_6H_6\subset\mathbf{2}$, (b) $CH_2Cl_2\subset\mathbf{2}$, (c) $DMSO\subset\mathbf{2}$, (d) $CHCl_3\subset\mathbf{2}$, and (e) $CCl_4\subset\mathbf{2}$.

crystals grown from toluene (V = 135 Å^3), C_6H_5F (V = 104 Å^3), and C_6H_5Cl (V = 129 Å^3) show that these solvents entered only at the extrinsic cavity and that the DMSO present at the intrinsic cavity of **2** remains undisturbed in all these instances. A similar conclusion can be arrived at from the MALDI-TOF mass spectra, which show the characteristic peaks due to $DMSO\subset\mathbf{2}$ in all these instances (Figures S26–S30, Supporting Information). Thus, it is apparent that guest molecules having volumes above 100 Å^3 are unable to enter the smaller intrinsic cavity and that **2** acts as a molecular flask that can separate benzene from other substituted benzene derivatives. Also **2** encapsulates cyclopentane over cyclohexane (V = 111.5 Å) due to its cavity size restrictions (Figures S22 and S30, Supporting Information). This is in contrast to the encapsulation observed for the water-soluble tetrahedral $Fe^{II}_4L_6$ cage assembly of Nitschke et al., which shows a tighter binding of cyclohexane over cyclopentane.[22] Also, it is interesting to note that the larger $[Ga_4L_6]^{12-}$ cage, reported by Raymond et al., can accommodate a range of n- and cycloalkanes by hydrophobic effect and specifically binds cyclodecane over n-decane in aqueous media.[23]

The selectivity of **2** for benzene and CCl_4 encapsulation over other competitive solvents such as CH_2Cl_2, $CHCl_3$, and C_5H_{10} was derived from mass spectral, NMR, and crystallographic analysis. Thus, treatment of $DMSO\subset\mathbf{2}$ with a mixture of equal amounts (0.5 mL) of all these five solvents gave $C_6H_6\subset\mathbf{2}$ as indicated by its characteristic peak centered at m/z = 2795 in the MALDI-TOF mass spectrum. Crystallographic experiments on the crystals (four different crystals were screened) grown from this solvent mixture confirm the exclusive formation of $C_6H_6\subset\mathbf{2}$. Also, the ^{1}H NMR of the obtained crystals in Me_2CO-d_6 showed a signal at δ = 7.32 ppm due to $C_6H_6\subset\mathbf{2}$. Analogous experiments with only chlorinated solvents showed

DOI: 10.1021/ic502798r
Inorg. Chem. 2015, 54, 3196–3202

the preferential encapsulation of CCl_4 over CH_2Cl_2 and $CHCl_3$ as observed from the mass spectrum (Figure 5 and Figure S31, Supporting Information).

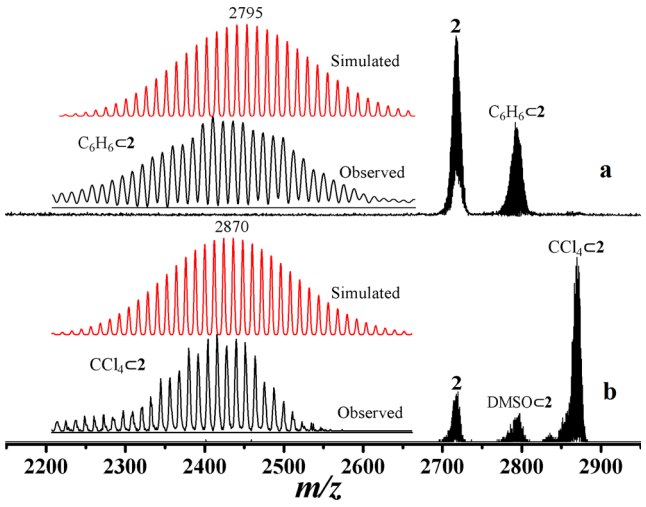

Figure 5. MALDI-TOF mass spectra of the samples of DMSO⊂**2** treated with a mixture of (a) benzene, CCl_4, CH_2Cl_2, $CHCl_3$, and C_5H_{10} and (b) only chlorinated solvents. (insets) The corresponding $[Guest⊂2+K]^+$ isotopic patterns.

Attempts to quantitatively estimate the guest binding abilities of **2** by ^1H NMR experiments were unsuccessful due to the unavailability of intracage host protons that can interact with the guest molecules and the negligible chemical shift differences between the free and bound guest solvents. Thus, the information pertaining to guest binding energies was derived from preliminary theoretical calculations by taking coordinates from the corresponding crystal structures. Among the host–guest complexes that are screened, $C_6H_6⊂2$ (−36.81 kcal/mol) shows more binding energy compared to other solvents as observed from Table 1. Of the three chlorinated solvents tested,

Table 1. Binding and Deformation Energies (kcal/mol) Calculated Using DFT/B97-D Level of Theory

complex	guest volume[24] (Å^3)	binding energy	deformation energy
DMSO⊂**2**	76.36	−36.11	0.47
C_6H_6⊂**2**	99.16	−36.81	0.32
CCl_4⊂**2**	88.69	−25.66	0.92
$CHCl_3$⊂**2**	74.68	−24.98	0.64
CH_2Cl_2⊂**2**	60.83	−22.50	0.78

CCl_4 is preferred over other solvents. This is attributed to (a) the symmetric shape of CCl_4 compared to others and (b) the volume compatibility[24] of CCl_4 with the host cage for efficient encapsulation. Also, the calculated deformation energies are below 1 kcal/mol for all the host–guest systems studied, which are too low to cause any significant distortion to the parent assembly. The TGA data of all the solvent encapsulated samples indicated that removal of the guest solvents did not destroy the cage assembly of **2** until 200 °C (Figure S32, Supporting Information). The cage assembly was also found to be stable in buffer solutions in the pH range between 3.5 and 9 as evidenced by ^{31}P NMR and mass spectral analyses (Figures S33 and S34, Supporting Information). Furthermore, the stable formation of **2** under competitive conditions was tested by reacting **1**·2DMSO with ferric oxalate, $Fe_2(C_2O_4)_3$, in methanol in which formation of DMSO⊂**2** was observed by MALDI-TOF and SC-XRD. Formation of the Pd-oxalate coordination against the Fe-oxalate bonds in this occasion demonstrates a remarkable stability for the cage structure of **2** (Scheme S2 and Figure S35, Supporting Information).

CONCLUSION

In conclusion, for the first time we have shown the formation of a charge-neutral tetrahedral Pd(II) cage assembly utilizing the $[Pd_3X]^{3+}$ cationic PBUs and linker oxalate anions. Although the imido P(V) moieties are well-documented for their coordination chemistry and catalysis,[25] use of these ligands as anionic cis-blocking agents in metallo-supramolecular cage chemistry has so far been unprecedented. However, the prismatic structure of the PBU precursor assemblies was retained when a monocarboxylate ion or a 0° clipping ferrocene dicarboxylate ion, which does not offer large-angle chelation, was employed in the ligand substitution reactions. Guest encapsulation inside **2** was examined for a large selection of solvents ranging from nonpolar to polar with the help of DOSY NMR, mass spectral, SC-XRD, and theoretical analyses. Also, preferential encapsulation of benzene and CCl_4 over other related aromatic and chlorinated solvents has been derived from mass spectral analysis. Currently, we are focusing on synthesizing other kinds of Platonic or Archimedean polyhedra utilizing these new found $[Pd_3X]^{3+}$ PBUs and various suitable linker ligands.

ASSOCIATED CONTENT

Supporting Information

Crystallographic information files and tables, spectra, cavity volume calculations, gas adsoption analysis, guest encapsulation studies, stability studies. This material is available free of charge via the Internet at http://pubs.acs.org.

AUTHOR INFORMATION

Corresponding Authors

*E-mail: boomi@iiserpune.ac.in. (R.B.)
*E-mail: cjeet@iiserpune.ac.in. (J.C.)

Notes

The authors declare no competing financial interest.

ACKNOWLEDGMENTS

This work was supported by DST (SR/S1/IC-50/2012), India, and IISER, Pune. A.Y. and S.N. acknowledge CSIR, India, for fellowship. We thank Dr. R. Vaidhyanathan for gas adsorption measurements and Dr. R. Natarajan and Dr. A. Venkatnathan for valuable discussions. We acknowledge the computing facilities provided by IISER, Pune, for theoretical studies.

DEDICATION

This paper is dedicated to Prof. V. Chandrasekhar for his contributions to the phosphorus chemistry.

REFERENCES

(1) (a) Lehn, J.-M. *Science* **2002**, *295*, 2400–2403. (b) Stoddart, J. F. *Nat. Chem.* **2009**, *1*, 14–15. (c) McKinlay, R. M.; Cave, G. W.; Atwood, J. L. *Proc. Natl. Acad. Sci. U. S. A.* **2005**, *102*, 5944–5948.
(2) (a) Hof, F.; Craig, S. L.; Nuckolls, C.; Rebek, J., Jr. *Angew. Chem., Int. Ed.* **2002**, *41*, 1488–1508. (b) Wieser, C.; Dieleman, C. B.; Matt, D. *Coord. Chem. Rev.* **1997**, *165*, 93–161. (c) Baldini, L.; Casnati, A.; Sansone, F.; Ungaro, R. *Chem. Soc. Rev.* **2007**, *36*, 254–266. (d) Szejtli, J. *Chem. Rev.* **1998**, *98*, 1743–1754. (e) Mecozzi, S.; Rebek, J., Jr.

DOI: 10.1021/ic502798r
Inorg. Chem. 2015, 54, 3196–3202

Chem.—Eur. J. **1998**, *4*, 1016−1022. (f) Liu, Y.; Hu, C.; Comotti, A.; Ward, M. D. *Science* **2011**, *333*, 436−440.
(3) (a) Pluth, M. D.; Bergman, R. G.; Raymond, K. N. *Science* **2007**, *316*, 85−88. (b) Swiegers, G. F.; Malefetse, T. J. *Chem. Rev.* **2000**, *100*, 3483−3538. (c) Wang, Z. J.; Clary, K. N.; Bergman, R. G.; Raymond, K. N.; Toste, F. D. *Nat. Chem.* **2013**, *5*, 100−103. (d) Ajami, D.; Rebek, J., Jr. *Proc. Natl. Acad. Sci. U. S. A.* **2007**, *104*, 16000−16003. (e) Schwarzmaier, C.; Schindler, A.; Heindl, C.; Scheuermayer, S.; Peresypkina, E. V.; Virovets, A. V.; Neumeier, M.; Gschwind, R.; Scheer, M. *Angew. Chem., Int. Ed.* **2013**, *52*, 10896−10899. (f) Mal, P.; Breiner, B.; Rissanen, K.; Nitschke, J. R. *Science* **2009**, *324*, 1697−1699. (g) Yoshizawa, M.; Klosterman, J. K.; Fujita, M. *Angew. Chem., Int. Ed.* **2009**, *48*, 3418−3438. (h) Clever, G. H.; Tashiro, S.; Shionoya, M. *Angew. Chem., Int. Ed.* **2009**, *48*, 7010−7012. (i) Cram, D. J.; Tanner, M. E.; Thomas, R. *Angew. Chem., Int. Ed.* **1991**, *30*, 1024−1027.
(4) (a) Cook, T. R.; Zheng, Y.-R.; Stang, P. J. *Chem. Rev.* **2012**, *113*, 734−777. (b) Pluth, M. D.; Bergman, R. G.; Raymond, K. N. *Acc. Chem. Res.* **2009**, *42*, 1650−1659. (c) Saalfrank, R. W.; Burak, R.; Breit, A.; Stalke, D.; Herbst-Irmer, R.; Daub, J.; Porsch, M.; Bill, E.; Müther, M.; Trautwein, A. X. *Angew. Chem., Int. Ed.* **1994**, *33*, 1621−1623. (d) Chakrabarty, R.; Mukherjee, P. S.; Stang, P. J. *Chem. Rev.* **2011**, *111*, 6810−6918. (e) Leininger, S.; Olenyuk, B.; Stang, P. J. *Chem. Rev.* **2000**, *100*, 853−908. (f) Fujita, M.; Tominaga, M.; Hori, A.; Therrien, B. *Acc. Chem. Res.* **2005**, *38*, 369−378. (g) Ronson, T. K.; Zarra, S.; Black, S. P.; Nitschke, J. R. *Chem. Commun.* **2013**, *49*, 2476−2490. (h) Ward, M. D.; Raithby, P. R. *Chem. Soc. Rev.* **2013**, *42*, 1619−1636. (i) Amouri, H.; Desmarets, C.; Moussa, J. *Chem. Rev.* **2012**, *112*, 2015−2041.
(5) (a) Stang, P. J.; Olenyuk, B. *Angew. Chem., Int. Ed.* **1996**, *35*, 732−736. (b) Fujita, M.; Oguro, D.; Miyazawa, M.; Oka, H.; Yamaguchi, K.; Ogura, K. *Nature* **1995**, *378*, 469−471. (c) Bar, A. K.; Raghothama, S.; Moon, D.; Mukherjee, P. S. *Chem.—Eur. J.* **2012**, *18*, 3199−3209. (d) Lu, Z.; Knobler, C. B.; Furukawa, H.; Wang, B.; Liu, G.; Yaghi, O. M. *J. Am. Chem. Soc.* **2009**, *131*, 12532−12533. (e) Mirtschin, S.; Slabon-Turski, A.; Scopelliti, R.; Velders, A. H.; Severin, K. *J. Am. Chem. Soc.* **2010**, *132*, 14004−14005. (f) Stephenson, A.; Argent, S. P.; Riis-Johannessen, T.; Tidmarsh, I. S.; Ward, M. D. *J. Am. Chem. Soc.* **2011**, *133*, 858−870.
(6) (a) Caulder, D. L.; Powers, R. E.; Parac, T. N.; Raymond, K. N. *Angew. Chem., Int. Ed.* **1998**, *37*, 1840−1843. (b) Caulder, D. L.; Raymond, K. N. *Acc. Chem. Res.* **1999**, *32*, 975−982. (c) Saalfrank, R. W.; Burak, R.; Breit, A.; Stalke, D.; Herbst-Irmer, R.; Daub, J.; Porsch, M.; Bill, E.; Müther, M.; Trautwein, A. X. *Angew. Chem., Int. Ed.* **1994**, *33*, 1621−1623. (d) Liu, G.; Ju, Z.; Yuan, D.; Hong, M. *Inorg. Chem.* **2013**, *52*, 13815−13817. (d) Clegg, J. K.; Li, F.; Jolliffe, K. A.; Meehan, G. V.; Lindoy, L. F. *Chem. Commun.* **2011**, *47*, 6042−6044.
(7) (a) Li, J. R.; Zhou, H. C. *Angew. Chem., Int. Ed.* **2009**, *48*, 8465−8468. (b) Li, J.-R.; Zhou, H.-C. *Nat. Chem.* **2010**, *2*, 893−898. (c) Ni, Z.; Yassar, A.; Antoun, T.; Yaghi, O. M. *J. Am. Chem. Soc.* **2005**, *127*, 12752−12753. (d) Chun, H. *J. Am. Chem. Soc.* **2008**, *130*, 800−801. (e) Liu, M.; Liao, W.; Hu, C.; Du, S.; Zhang, H. *Angew. Chem., Int. Ed.* **2012**, *51*, 1585−1588. (f) Bi, Y.; Wang, X.-T.; Liao, W.; Wang, X.; Wang, X.; Zhang, H.; Gao, S. *J. Am. Chem. Soc.* **2009**, *131*, 11650−11651. (g) Tan, H.; Du, S.; Bi, Y.; Liao, W. *Chem. Commun.* **2013**, *49*, 8211−8213. (h) Zheng, S.-T.; Zhang, J.; Li, X.-X.; Fang, W.-H.; Yang, G.-Y. *J. Am. Chem. Soc.* **2010**, *132*, 15102−15103.
(8) (a) Murray, C. A.; Cardin, C. J.; Greenland, B. W.; Swift, A.; Colquhoun, H. M. *Inorg. Chem.* **2013**, *52*, 10424−10430. (b) Li, J.-R.; Yu, J.; Lu, W.; Sun, L.-B.; Sculley, J.; Balbuena, P. B.; Zhou, H.-C. *Nat. Commun.* **2013**, *4*, 1538.
(9) (a) Leininger, S.; Olenyuk, B.; Stang, P. J. *Chem. Rev.* **2000**, *100*, 853−908. (b) Seidel, S. R.; Stang, P. J. *Acc. Chem. Res.* **2002**, *35*, 972−983. (c) Fujita, M.; Tominaga, M.; Hori, A.; Therrien, B. *Acc. Chem. Res.* **2005**, *38*, 369−378. (d) Fujita, M.; Umemoto, K.; Yoshizawa, M.; Fujita, N.; Kusukawa, T.; Biradha, K. *Chem. Commun.* **2001**, 509−518.
(10) Gupta, A. K.; Reddy, S. A. D.; Boomishankar, R. *Inorg. Chem.* **2013**, *52*, 7608−7614.
(11) Sheldrick, G. M. *Acta Crystallogr.* **2008**, *A64*, 112−122.
(12) Wu, D.; Chen, A.; Johnson, C. S., Jr. *J. Mag. Reson., Ser. A* **1995**, *115*, 260−264.
(13) Kerssebaum, R. DOSY and Diffusion by NMR. In *Users Guide for XWinNMR 3.5,* Version 1.0; Bruker BioSpin GmbH: Rheinstetten, Germany, 2002.
(14) Grimme, S. *J. Comput. Chem.* **2006**, *27*, 1787−1799.
(15) Frisch, M. J. et al. *Gaussian 09,* Revision C.01; Gaussian, Inc.: Wallingford, CT, 2010.
(16) Ramya, K. R.; Venkatnathan, A. *Comput. Theor. Chem.* **2013**, *1023*, 1−4.
(17) Leininger, S.; Fan, J.; Schmitz, M.; Stang, P. J. *Proc. Natl. Acad. Sci. U. S. A.* **2000**, *197*, 1380−1384.
(18) (a) Connolly, M. L. *J. Mol. Graphics* **1993**, *11*, 139−141. (b) Barbour, L. J. *Chem. Commun.* **2006**, 1163−1168.
(19) (a) Lawrence, S.; Williams, D. *Chem. Commun.* **1997**, 285−286. (b) Mingos, D. M. P.; Vilar, R. *J. Organomet. Chem.* **1998**, *557* (1), 131−142. (c) Vilar, R.; Michael, D.; Mingos, P. *J. Cluster Sci.* **1996**, *7*, 663−675.
(20) (a) Mukherjee, P. S.; Das, N.; Kryschenko, Y. K.; Arif, A. M.; Stang, P. J. *J. Am. Chem. Soc.* **2004**, *126*, 2464−2473. (b) Bar, A. K.; Gole, B.; Ghosh, S.; Mukherjee, P. S. *Dalton Trans.* **2009**, 6701−6704. (c) Bar, A. K.; Shanmugaraju, S.; Chi, K.-W.; Mukherjee, P. S. *Dalton Trans.* **2011**, *40*, 2257−2267.
(21) A small amount of NaI is added to obtain a well-resolved $[CH_2Cl_2 \subset \mathbf{2}+Na]^+$ ion signal.
(22) Mal, P.; Schultz, D.; Beyeh, K.; Rissanen, K.; Nitschke, J. R. *Angew. Chem., Int. Ed.* **2009**, *47*, 8297−8301.
(23) Biros, S. M.; Bergman, R. G.; Raymond, K. N. *J. Am. Chem. Soc.* **2007**, *129*, 12094−12095.
(24) Ronson, T. K.; Giri, C.; Beyeh, N. K.; Minkkinen, A.; Topić, F.; Holstein, J. J.; Rissanen, K.; Nitschke, J. R. *Chem.—Eur. J.* **2013**, *19*, 3374−3382.
(25) (a) Chivers, T.; Hilts, R. W. *Coord. Chem. Rev.* **1994**, *137*, 201−232. (b) Beswick, M. A.; Wright, D. S. *Coord. Chem. Rev.* **1998**, *176*, 373−406. (c) Steiner, A.; Zacchini, S.; Richards, P. I. *Coord. Chem. Rev.* **2002**, *227*, 193−216. (d) Buchard, A.; Auffrant, A.; Klemps, C.; Vu-Do, L.; Boubekeur, L.; Le Goff, X. F.; Le Floch, P. *Chem. Commun.* **2007**, 1502−1504. (e) Rastätter, M.; Zulys, A.; Roesky, P. W. *Chem. Commun.* **2006**, 874−876. (f) Dehnicke, K.; Weller, F. *Coord. Chem. Rev.* **1997**, *158*, 103−169. (g) Dehnicke, K.; Krieger, M.; Mass, W. *Coord. Chem. Rev.* **1999**, *182*, 19−65.

DOI: 10.1021/ic502798r
Inorg. Chem. 2015, 54, 3196−3202